scientific reports

OPEN

Method of bed exit intention based on the internal pressure features in array air spring mattress

Fanchao Meng[1,2,3], Teng Liu[1,2,3✉], Chuizhou Meng[1,2,3], Jianjun Zhang[1,2,3], Yifan Zhang[4] & Shijie Guo[1,2,3]

With the population ages, many patients are unable to receive comprehensive care, leading to an increase in hazardous incidents, particularly falls occurring after getting out of bed. To address this issue, this paper proposes a method for recognizing bed-exit intentions using an array air spring mattress. The method integrates convolutional neural networks with feature point matching techniques to identify both global and local features of the array air spring. For global features, a one-dimensional focal loss convolutional neural network (1D-FLCNN) model is employed to classify eight internal pressure time series and determine bed-exit status based on global features. For local features, the distribution matrix and feature point matrix of the internal pressure features are extracted to represent the spatial distribution of bed-exit postures. Euclidean distance is utilized to measure the similarity between these matrices and match bed-exit postures. Finally, the recognition results from both feature types are combined using a logical OR operation to produce the final result. Experimental validation confirms that the proposed method greatly improves the anti-interference capability and effectively avoids the problem of non-recognition due to body position and external environment.

The process of getting out of bed in older adults is a common stage for falling incidents[1–3], which can lead to traumatic brain injury (TBI) and soft tissue injury (STI)[4]. Falls are the second leading cause of unintentional injury deaths worldwide, presenting a significant health risk for the elderly[5,6]. Therefore, it is essential to promptly alert caregivers or family members if an elderly individual at high risk of falling is observed sitting up or attempting to leave the bed, as this can help prevent falls[7,8]. Although air spring mattresses are widely used in nursing, research on their effectiveness in health tracking, auxiliary technologies, and sleep posture recognition remains limited[9–11]. Moreover, studies on detecting bed-exit intention are scarce. This paper proposes a method for identifying bed-exit intention using an air spring mattress equipped with air pressure sensors. This research is both important and urgent, as it can provide valuable technical support to enhance patient care and quality of life.

Current research on bed-exit intention recognition in the nursing field primarily focuses on monitoring changes in global and local features. Global and local features are distinguished based on their scope and the level of information they provide.

Generally, global features primarily include pressure image[12], temperature distribution[13], visual surveillance[14,15] and pressure distribution[16]. For example, Lin et al[17]. developed a low-complexity system that monitors out-of-bed activities by analyzing a series of narrow-field images. Gutierrez et al[18]. created a body posture monitoring system using far-infrared (FIR) images, which uses the relative motion of body joints to monitor out-of-bed posture. Inoue et al[19]. employed long short-term memory (LSTM) to differentiate bed-exit movements from other types of movements. Zhang et al[20]. designed a multi-parameter passive wireless flexible sensor (MPWFS) to monitor pressure and temperature, using an array to track off-bed postures. Valero et al[21]. developed a health and sleep care assistant that uses intelligent sensors to detect bed vibrations during physical activities and continuously monitor bed activity. Monitoring global features[22,23] for recognizing human behavior

[1]Engineering Research Center of the Ministry of Education for Intelligent Rehabilitation Equipment and Detection Technologies, Hebei University of Technology, Tianjin 300130, China. [2]Hebei Key Laboratory of Smart Sensing and Human-Robot Integration, Hebei University of Technology, Tianjin 300130, China. [3]School of Mechanical Engineering, Hebei University of Technology, Tianjin 300130, China. [4]School of Computer Science and Technology, Civil Aviation University of China, Tianjin 300300, China. ✉email: wuqiu-liu@163.com
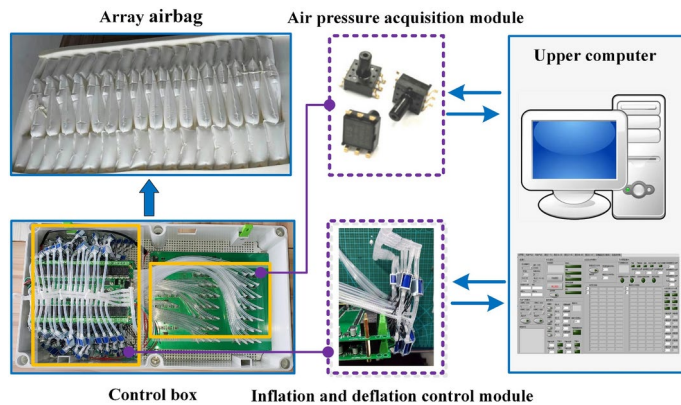
Fig. 1. Array air spring mattress platform.
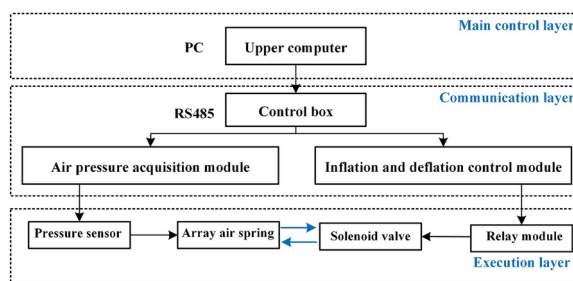
Fig. 2. Structure of array air spring mattress.

offers several advantages, such as high accuracy, non-invasiveness, and real-time capability. However, it also has certain limitations, including reduced granularity and susceptibility to environmental factors.

Local features commonly used in intention recognition include localized temperature[24], switch signals[25], angle signals, localized pressure distribution[26,27] and sound signals. For example, Ruiz et al[28]. developed an out-of-bed posture monitoring system using an inertial measurement unit (IMU) and three pressure sensors, capable of recognizing three types of lying postures and transitions between sitting in bed and sitting bedside. Lin et al[29]. proposed a in/out of bed posture monitoring system based on a chest-worn wearable device, which uses a triaxial accelerometer and gyroscope within a nine-axis inertial sensor to determine the user's posture. Woltsche et al[30]. employed portable video monitors (PVM) to identify out-of-bed posture by detecting noise generated from patient movements and alerting caregivers through the sound on the screen. Monitoring local features offers advantages such as privacy protection, diversity, and adaptability, but it also faces challenges including incomplete information and susceptibility to body position.

From the current research, it is evident that bed-exit intention recognition is primarily limited to either global or local feature recognition. Single-feature recognition is prone to environmental and body position-related errors. For this problem, the paper proposed a bed-exit intention recognition method based on the time series[31] and the feature points matching of air spring internal pressure to identify the dangerous state of bed-exit intention, which can effectively avoid the problem of incorrect recognition due to the environment and body position.

Materials and methods
Air spring mattress platform
In this paper, an array air spring mattress experimental platform was constructed independently for experimental data acquisition, as depicted in Fig. 1. The platform comprises 67 air springs, each connected to an individual air pressure sensor. To enhance the mattress's comfort, a diagonal wedge configuration was employed for the middle two columns of air springs, resulting in 17 air springs in one column and 16 in the other.

The platform is structured into three layers: the main control layer, the communication layer, and the execution layer, as illustrated in Fig. 2. Figure 3(a) presents the pneumatic diagram of the mattress control system, showing the connections between the pressure sensor, solenoid valve, air spring, air pump, and gas holder. Data filtering in this study was performed using digital techniques within the signal acquisition circuitry. A low-pass filter was initially applied to mitigate high-frequency noise, such as tremors from bedridden patients. For data preprocessing, a sliding window with a time step of 1 was used, and median filtering was selected as the filtering method. After applying both the low-pass filter and median filtering, stable sensor data were obtained. The results of the data filtering are shown in Fig. 3(b).
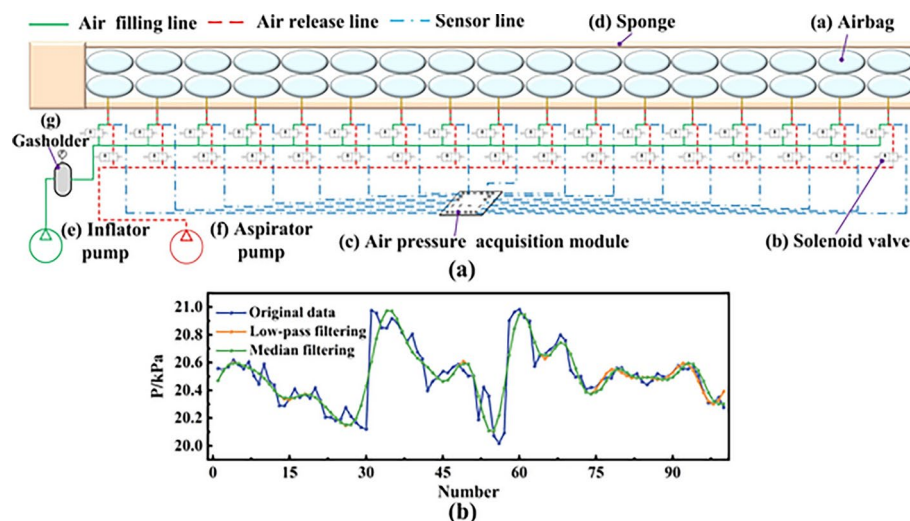
Fig. 3. Air spring mattress pneumatic system and data filtering (**a**) pneumatic system (**b**) the data filtering results.
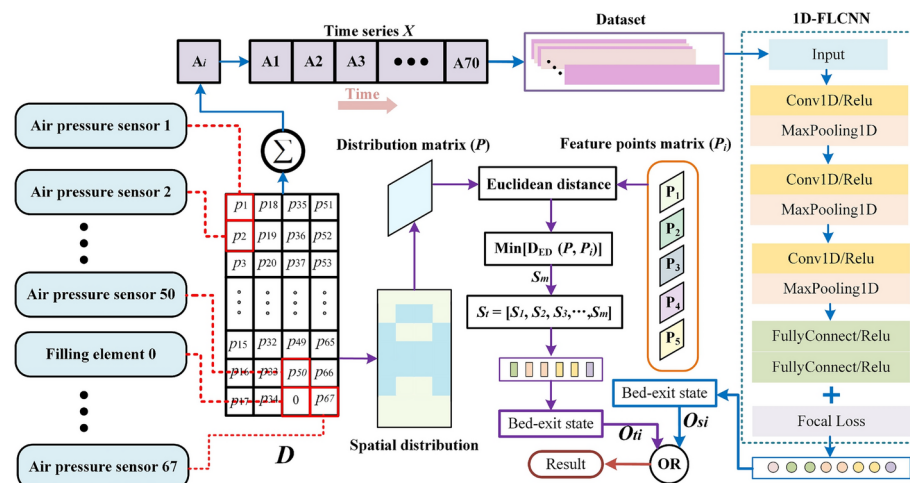
Fig. 4. Overall framework.

Research method

In elderly care, specific postures including sitting in bed, sitting at bedside, transitioning from a supine position to sitting, and turning back serve as critical indicators for monitoring the bed-exit intentions[32,33]. By observing the occurrence or changes in these postures, the bed-exit intention of the elderly individual can be analyzed. Figure 4 illustrates the overall framework of the method. The detailed algorithm flow is given in Algorithm1.

Input: internal pressure distribution D
Output: Out
1: **while** internal pressure distribution D is not empty
2: // Global feature part
3:    A = Sum (D) // A is in Eq. (4)
4:    X = Construct_internal_pressure_time_sequence (A) // X is in Eq. (5)
5:    X_T = Normalization (X) // X_T is in Eq. (6)
6:    Pre = 1D_FLCNN_model.predict (X_T)
7:    O_s = Judge_predicted_posture (Pre)// O_s is the four bed-exit intention dangerous
        states
8: // Local feature part
9:    P = Posture_distribution_matrix(D) // P is in Eq. (8)
10:    S_m= Min_Euclidean_distance (P, P_i), i=1,2,3,4,5 // P_i in Eq. (10)-(14), S_m in Eq. (15)
11:    S_t = Form_posture_sequence (S_m) // S_t is in Eq. (16)
12:    O_t= judge_posture_sequence (S_t) // O_t is the four bed-exit intention dangerous states
13:// Bed-exit intention recogniction
14:    Out=Logic_or (O_s, O_t) // Logic_or is given in Eq. (1)
15:    D=empty
16: **end while**
17: **return** Out

Algorithm 1 Method of bed-exit intention based on the global and local features.

The method contains two main parts. On the one hand, the 1D-FLCNN model is utilized to explore the time series and bed-exit posture mapping relationship of the air spring internal pressure distribution. On the other hand, the spatial distribution of the internal pressure is further employed to extract the feature points matrix based on the distribution properties of the human body load to obtain a better local feature expression, and the Euclidean distance is used for feature point matching. The two parts of recognition results are integrated through logical OR operation to output the result. The details are as follows.

(1) Global feature (Time series).

The single-point total pressure data are organized chronologically to form an internal pressure time series. This dataset is randomly divided into training and testing sets for training a 1D-FLCNN classification model. The model is trained to identify eight internal pressure time series, namely lie-down, sitting in bed, sitting in bedside, nobody, backpart-lifting, turn-back, out of bed, and fall bed. The time series are divided into four dangerous states of the bed-exit intention. Falling out of bed is determined if the recognized time series indicates fall bed. A general intention to get out of bed is inferred if the identification shows sitting in bed and backpart-lifting. A strong intention to get out of bed is discerned when it is recognized as sitting in bedside and turn-back. Finally, getting out of bed is concluded if it is identified as out of bed and nobody.

(2) Local features (Feature points matching).

Firstly, the distribution matrix of the internal pressure features spatial distribution of bed-exit posture is extracted. Then, based on the threshold of bed-exit posture distribution matrix, the feature points matrix is obtained. Euclidean distance measures the similarity between the distribution matrix and the feature points matrix to match five postures: lie-down, backpart-lifting, right turn-back, left turn-back and out of bed. Next, the similarity results form a posture sequence, which is analyzed to determine the order of bed-exit postures. Sequences are interpreted as follows: a progression from lie-down to out of bed indicates a fall; lie-down to backpart-lifting suggests a general intention to get out of bed; lie-down to backpart-lifting to right/left turn-back indicates a strong intention; and lie-down, backpart-lifting, right/left turn-back, out of bed confirms that the user has exited the bed. Other sequences do not trigger alerts.

Ultimately, the two parts of recognition results are integrated through logical OR operation to output the result. The calculation logic is described in Eq. (1).

$$O_{si}|O_{tj} = \begin{cases} O_{si} , & i \leq j \\ O_{tj} , & i > j \end{cases} \quad (i,j = 1,2,3,4) \tag{1}$$

where O_{s1}, O_{s2}, O_{s3}, O_{s4} and O_{t1}, O_{t2}, O_{t3}, O_{t4} respectively represent the four bed-exit intention dangerous states of falling out of bed, leaving the bed, strong intention, and general intention to get out of bed identified by the global and local feature part.

4

Based model
1D-FLCNN

The time series of air spring internal pressure typically exhibits characteristics such as multiple parameter correlations and dynamic variations, which makes feature extraction challenging. The 1D-CNN model effectively matches these data characteristics due to its simple structure, strong feature extraction capabilities, and efficient computational performance. Compared to other more complex models, the 1D-CNN model is better suited for handling time series data and extracting essential features. This paper utilizes the feature extraction capability of 1D-CNN and the attention to difficult-to-distinguish samples of FL to achieve accurate classification of internal pressure series.

In traditional 1D-CNN[34–36] model, square error or cross-entropy is commonly used as the loss function for classification, treating each category in the dataset equally without considering variations in sample difficulty. To enhance classification accuracy, this paper employs the FL function instead of conventional cross-entropy loss. The FL function increases the misclassification weight of difficult samples and decreases that of normal samples, thereby improving the model's focus on challenging cases. Based on this, the 1D-FLCNN sample classification model is proposed.

Focal Loss (FL), proposed by Lin et al[37]. to address the issue of class imbalance in object detection, enhances the standard cross-entropy loss function. Its main idea is to reduce the weight of easily classified samples, enabling the model to prioritize challenging samples during training. For an m-class problem with a total of n training samples, the cross-entropy loss can be represented as Eq. (2).

$$L = -\sum_{i=1}^{n}\sum_{j=1}^{m} y_j^i \log_2 p_j^i = -\sum_{i=1}^{n} \log_2 p_j^i \qquad (2)$$

where p_j^i represents the probability of sample i being predicted as class j, and y_j^i denotes the true class label of that sample.

The 1D-FLCNN model structure in this paper is shown in Fig. 4. The front-end network consists of three alternating convolution and pooling layers, and the back-end network connects two fully connected layers. The convolution layer can extract deeper features of signals, and a pooling layer is added after each convolution layer to reduce the data dimension and improve the training efficiency. The fully connected layer maps data features into a one-dimensional vector to input to the classifier. When calculating the classification loss, different classification weights are assigned to challenging samples and normal class samples by setting the values of parameters α and γ in the Focal Loss. The accurate recognition of various types of samples is achieved through the powerful feature extraction capability of 1D-CNN and the attention given to challenging samples by Focal Loss.

Feature points matching

The feature point matching method proposed in this paper considers the distribution matrix of posture pressure features and the feature point matrix. It employs the Euclidean distance to measure similarity, enabling accurate matching of bed-exit postures and comprehensive analysis of posture sequences for status determination.

Pattern matching involves two main steps: feature extraction and similarity measurement. Feature extraction reduces the data dimension by transforming the original data to extract the most relevant information. Similarity measurement takes the reduced-dimension feature sequences as input and calculates the distance between two sequences by the distance measurement formula. The smaller distance indicates the higher similarity between the two sequences. Common pattern matching methods include dynamic time warping (DTW[38]), Euclidean distance (ED[39]), and singular value decomposition (SVD[40]), among others.

For general generality, the similarity between the distribution matrix P of real-time postures and the feature points matrices P_i of the bed-exit postures is assessed using the square of the Euclidean distance. This method is widely applied in the fields of pattern recognition and feature matching due to its effectiveness in handling continuous data and high-dimensional spaces. The Euclidean distance algorithm is straightforward, easy to understand, and implement, making it versatile for various application scenarios. The equation is as follows:

$$D_{ED}(P, P_i) = \sum_{j=1}^{4}\sum_{h=1}^{4} [P(j,h) - P_i(j,h)]^2 \qquad (3)$$

where $P(j, h)$ and $P_i(j, h)$ are the elements on row j and column h of P and P_i, respectively.

Experimental design
Time series data collection experiment

The time series data collection experiment is described in Fig. 5. The participants lie on the array air spring mattress to conduct the experiment. Due to the uncertainty in the participant's bed-exit intention state while on the bed, long-term data monitoring is required. In this paper, video recordings and marking method is employed to extract internal pressure time series dataset. The dataset creation process involves two main steps. First, participant behavior on the bed is recorded via video surveillance, with corresponding internal pressure time series data captured simultaneously. The video recordings and internal pressure time series data share the same time stamps. Second, the video segments are replayed, and the collected internal pressure time series data
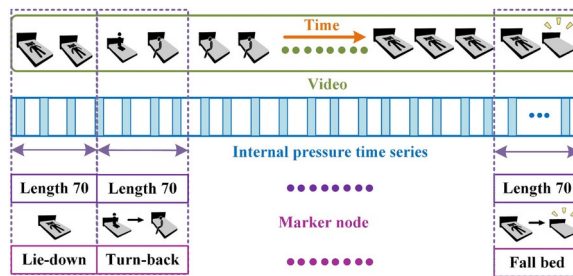
Fig. 5. Time series data acquisition experiment.

are segmented and labeled at consistent time intervals according to these time stamps. The labels correspond to the participant's postures on the array air spring mattress, resulting in a labeled dataset after segmentation. The testing set is a subset of the dataset, randomly selected for evaluating the model's performance. The study involved a total of 30 participants, generating 4800 sets of data, with 600 sets for each of the eight-time series. In this paper, 70% of the time series dataset was allocated for training, 15% for validation, and the remaining 15% for testing.

The sensing of internal pressure in the mattress is accomplished using 67 sensors. The pressure values from each air spring are summed, and the resulting total pressure data are arranged in chronological order to form an internal pressure time series. This time series consists of 70 transient total pressures collected over a period of 3 s. To ensure consistency, the time series is normalized. The treatment formula is

$$A_i = \sum_{i=1}^{67} p_i \tag{4}$$

$$X = [A_1, A_2, A_3, ..., A_{70}] \tag{5}$$

$$X_T = \frac{X - X.\min}{X.\max - X.\min} \tag{6}$$

where A_i is the transient total pressure, X is the internal pressure series, $X.$min is the minimum value of X, $X.$max is the maximum value of X, X_T is a one-dimensional array after normalization.

The randomly selected preprocessed time series samples are illustrated in Fig. 6. Among them, (a), (b), (c), and (d) represent the time series of participants in a single posture. Conversely, (e), (f), (g), and (h) represent the time series of participants in variable postures. The x-axis represents the sequential numbering of time series points, while the y-axis represents normalized internal pressure values.

Feature points extracting experiment

The air pressure perception experiments were performed to obtain the spatial distribution of the load of the bed-exit posture on the air spring mattress. According to the spatial distribution of posture load and the degree of correlation, the interference of secondary information was eliminated, and the real-time pressure distribution matrix D was integrated into a distribution matrix P. Subsequently, a threshold-based method was then used to extract internal pressure distribution feature points from regions covered by the distribution matrix for each bed-exit posture. These feature points were then incorporated into the distribution matrix P to form the feature points matrix P_i. The feature matrix represents the postures: lie-down, backpart-lifting, right turn-back, left turn-back, and out-of-bed.
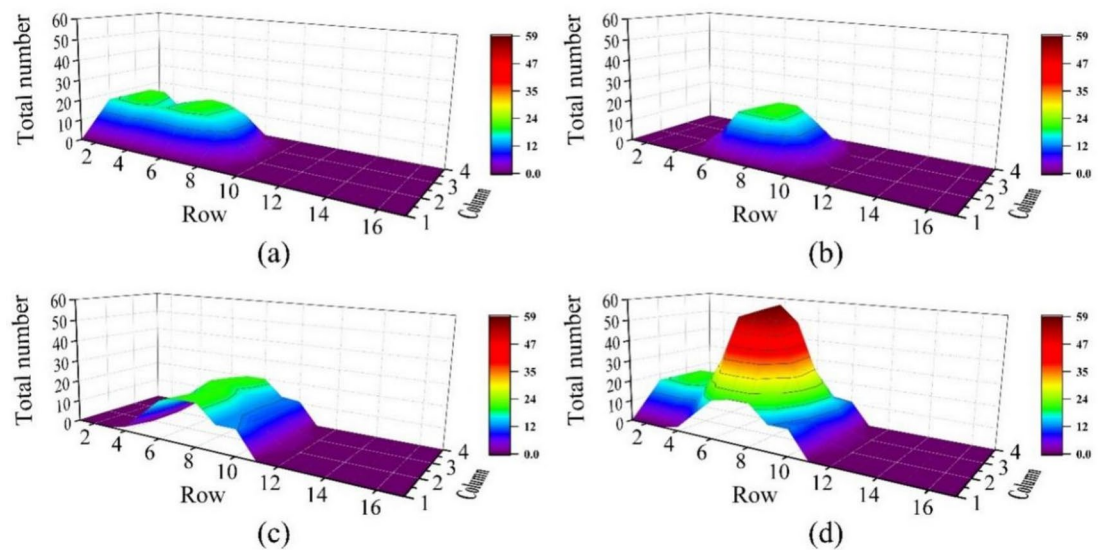
The air pressure perception experiments involved 20 male and female participants, who provided data on internal pressure distribution for various bed-exit postures. Significant changes in pressure distribution from the initial state were analyzed, with regions exhibiting prominent pressure changes being extracted.

The findings of air pressure perception experiments are illustrated in Fig. 7. The x-axis denotes the row number of the air spring array, the y-axis represents the column number, and the z-axis indicates the number of participants exhibiting significant pressure changes. Figure 7(a) shows notable variations in pressure distribution within the back and hip regions for the lie-down posture. Figure 7(b) highlights pronounced changes in the hip region for the backpart-lifting posture. Figure 7(c) shows notable variations in pressure distribution within the hip and its lateral regions in the right/left turn-back posture. Figure 7(d) combines the results from (a), (b), and (c) to present the integrated spatial distribution of bed-exit postures on the array air spring mattress. For the out-of-bed, the distribution features do not require statistical analysis since they are identical to the initial state. The spatial distribution of the bed-exit postures can be represented by combining the air springs' combinations at specific positions listed in Table 1.

To ensure the integrity and effectiveness of the real-time internal pressure matrix D, a supplementary element of 0 is utilized to fill in missing elements. This supplementary value does not impact the proposed method and can be any numerical value. Figure 8(a) illustrates the process of extracting the distribution matrix P, with the numbers indicating the air spring positions, which correspond to the pressure sensors.
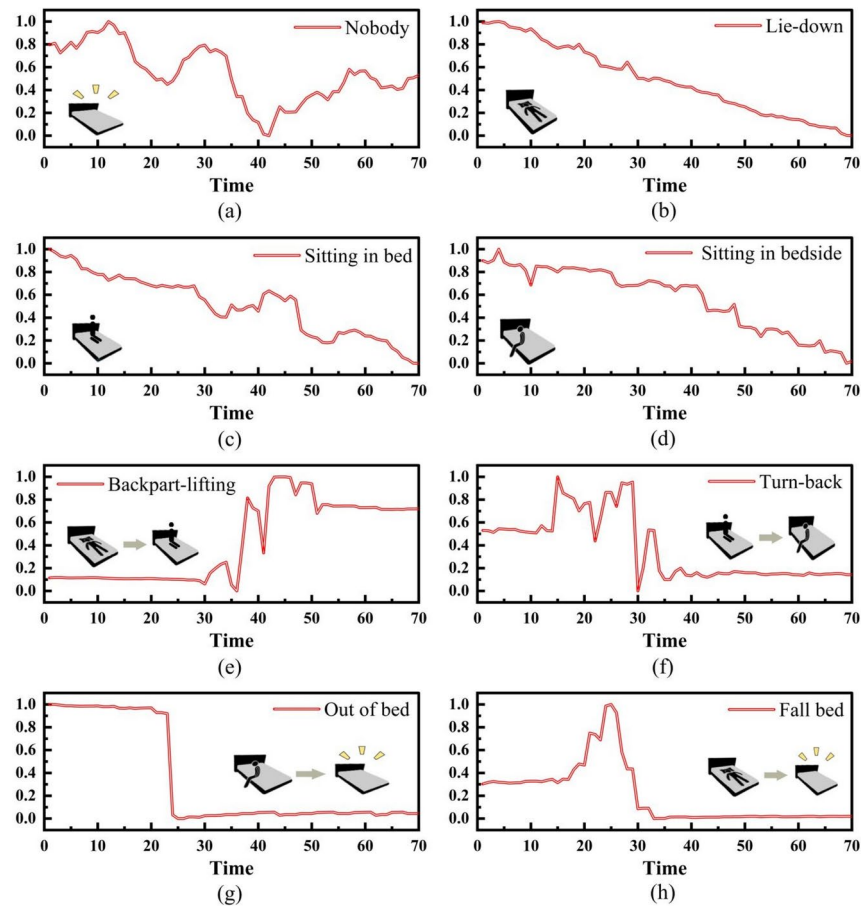
Fig. 6. Samples of each time series.

Fig. 7. The findings of air pressure perception experiments (**a**) Lie-down (**b**) Backpart-lifting (**c**) Right/Left turn-back (**d**) Sum of postures.

Posture	Spatial distribution
Lie-down	Air spring 20, 23, 36, 40
Backpart-lifting	Air spring 24, 25, 41,42
Right turn-back	Air spring 24, 25, 7, 8, 4, 5, 6, 9, 10
Left turn-back	Air spring 40, 41, 57, 58, 54, 55, 56, 59, 60
Out-of-bed	All the above air springs

Table 1. The spatial distribution of the load of the bed-out posture.
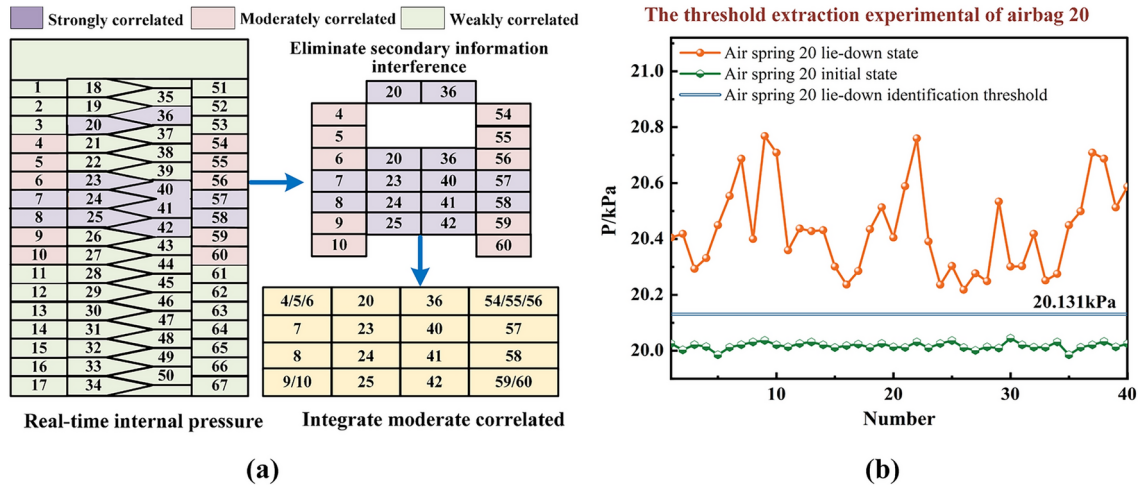
Fig. 8. Feature points extracting (**a**) schematic diagram of the distribution matrix P extraction (**b**) the threshold extraction experimental of airbag 20.

$$D = \begin{bmatrix} p_1 & p_{18} & p_{35} & p_{51} \\ p_2 & p_{19} & p_{36} & p_{52} \\ \dots & \dots & \dots & \dots \\ p_{16} & p_{33} & p_{50} & p_{66} \\ p_{17} & p_{34} & 0 & p_{67} \end{bmatrix} \tag{7}$$

$$P = \begin{bmatrix} a_{11} & a_{12} & a_{13} & a_{14} \\ a_{21} & a_{22} & a_{23} & a_{24} \\ a_{31} & a_{32} & a_{33} & a_{34} \\ a_{41} & a_{42} & a_{43} & a_{44} \end{bmatrix} = \begin{bmatrix} \frac{p_4+p_5+p_6}{3} & p_{20} & p_{36} & \frac{p_{54}+p_{55}+p_{56}}{3} \\ p_7 & p_{23} & p_{40} & p_{57} \\ p_8 & p_{24} & p_{41} & p_{58} \\ \frac{p_9+p_{10}}{2} & p_{25} & p_{42} & \frac{p_{59}+p_{60}}{2} \end{bmatrix} \tag{8}$$

where p_1, p_2 … p_{67} is the internal pressure value of the array air spring, D is internal pressure distribution of the array air spring mattress, P is the distribution matrix.

Following the extraction of the distribution matrix P, threshold experiments were conducted under the working state of the air springs, collecting the internal pressure values before and after each bed-exit posture. Due to limited space, only the threshold experimental results of the airbag 20 in the lie-down posture are presented in Fig. 8 (b). The x-axis represents the sequence number of the threshold extraction experiment, and the y-axis represents the internal pressure value. The threshold extraction formula is shown as Eq. 9.

$$T = \frac{L_s.\min - F_s.\max}{2} + F_s.\max \tag{9}$$

where $L_s.\min$ is the minimum internal pressure value of each behavior state, $F_s.\max$ is the maximum internal pressure value of the initial state of each behavior, T is the threshold of each behavior.

The thresholds extracted from the experiments are defined as feature points. The thresholds obtained from these experiments are defined as feature points, which are then applied to the distribution matrix to create the feature matrix P_i. The feature matrix represents the postures: lie-down, backpart-lifting, right turn-back, left turn-back, and out-of-bed. The corresponding feature points matrices are demonstrated in Eqs. 10–14. All the non-p_0 elements in the matrix are the corresponding feature point, and p_0 is the initial standard internal pressure.

$$P_1 = \begin{bmatrix} p_0 & p_{20}^{l} & p_{36}^{l} & p_0 \\ p_0 & p_{23}^{l} & p_{40}^{l} & p_0 \\ p_0 & p_0 & p_0 & p_0 \\ p_0 & p_0 & p_0 & p_0 \end{bmatrix} \tag{10}$$

$$P_2 = \begin{bmatrix} p_0 & p_0 & p_0 & p_0 \\ p_0 & p_0 & p_0 & p_0 \\ p_0 & p_{24}^{b} & p_{41}^{b} & p_0 \\ p_0 & p_{25}^{b} & p_{42}^{b} & p_0 \end{bmatrix} \tag{11}$$

$$P_3 = \begin{bmatrix} p_{re1}^{rt} & p_0 & p_0 & p_0 \\ p_7^{rt} & p_0 & p_0 & p_0 \\ p_8^{rt} & p_{24}^{rt} & p_0 & p_0 \\ p_{re2}^{rt} & p_{25}^{rt} & p_0 & p_0 \end{bmatrix} \tag{12}$$

$$P_4 = \begin{bmatrix} p_0 & p_0 & p_0 & p_{le1}^{lt} \\ p_0 & p_0 & p_{40}^{lt} & p_{57}^{lt} \\ p_0 & p_0 & p_{41}^{lt} & p_{58}^{lt} \\ p_0 & p_0 & p_0 & p_{le2}^{lt} \end{bmatrix} \tag{13}$$

$$P_5 = \begin{bmatrix} p_0 & p_0 & p_0 & p_0 \\ p_0 & p_0 & p_0 & p_0 \\ p_0 & p_0 & p_0 & p_0 \\ p_0 & p_0 & p_0 & p_0 \end{bmatrix} \tag{14}$$

where P_1 is the lie-down feature points matrix, p_{20}^{l}, p_{23}^{l}, p_{36}^{l}, p_{40}^{l} are the feature points of internal pressure distribution in lie-down, P_2 is the backpart-lifting feature points matrix, p_{24}^{b}, p_{25}^{b}, p_{41}^{b}, p_{42}^{b} are the feature points of internal pressure distribution in backpart-lifting, P_3 is the right turn-back feature points matrix, p_{re1}^{rt}, p_7^{rt}, p_8^{rt}, p_{re2}^{rt}, p_{24}^{rt}, p_{25}^{rt} are the feature points of internal pressure distribution in right turn-back, P_4 is the left turn-back feature points matrix, p_{le1}^{lt}, p_{57}^{lt}, p_{58}^{lt}, p_{le2}^{lt}, p_{40}^{lt}, p_{41}^{lt} are the feature points of internal pressure distribution in left turn-back, P_5 is the out-of-bed feature points matrix, p_0 is the initial standard internal pressure.

Results and analysis
Global feature
The 1D-FLCNN classification model is trained using the Adam optimizer, with a Batch size of 64. The learning rate is set to 0.001, and it iterates 200 times. Setting the value of parameter α in Focal Loss to 1 and setting the γ value based on empirical values as 2 can increase the misclassification weight for challenging samples. The specific parameters for the classification model are presented in Table 2. In this table, the convolution layer parameters are denoted within parentheses as follows: input channel, output channel, convolution kernel size, and step size. The pooling layer parameters consist of the pooling kernel size and step size. Additionally, the full-connection layer parameters, also enclosed in parentheses, indicate the number of nodes in the previous layer and the current layer.

To evaluate the effectiveness of the 1D-FLCNN model in recognizing each time series, the confusion matrix of the testing set results is examined, as depicted in Fig. 9 (a). Accuracy, derived from the confusion matrix, is defined as the ratio of correctly predicted instances to the total number of instances in the dataset. With only 4 misclassified samples out of 720 in the test set, the accuracy rate is 99.44%. To further validate the effectiveness of the 1D-FLCNN model in recognizing bed-exit intention time series, both the training set and testing set

Structure	Key parameter
Input	—
Conv1D + Relu	(1, 32, 1, 1)
MaxPooling1D	(2, 2)
Conv1D + Relu	(32, 64, 1, 1)
MaxPooling1D	(2, 2)
Conv1D + Relu	(64, 128, 1, 1)
MaxPooling1D	(2, 2)
Fully connected + Relu	(1024, 128)
Fully connected + Relu	(128, 8)

Table 2. Parameter setup of 1D-FLCNN.

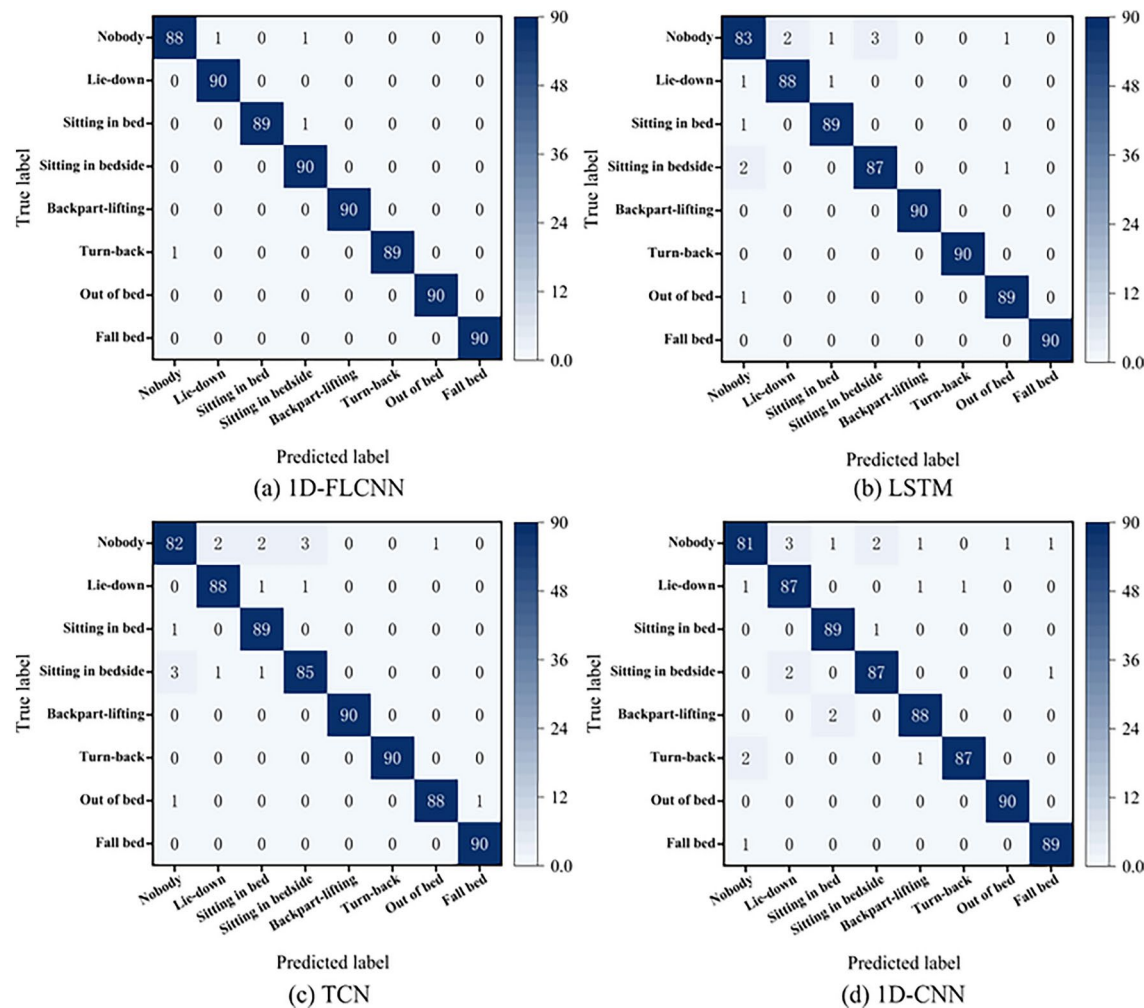**Fig. 9**. Testing set confusion matrix comparison of different classification models.

| Classification model	Testing set accuracy
1D-FLCNN	99.44%
LSTM	98.05%
TCN	97.50%
1D-CNN	96.94%

Table 3. Accuracy of different models on the testing set.

are utilized for comparison with other models: Long Short-Term Memory (LSTM), Temporal Convolutional Network (TCN) and 1D-CNN. The recognition results of each model's testing set are presented in Table 3.

The testing set confusion matrix comparison of different classification models are shown in Fig. 9. The y-coordinate represents the real category, and the x-coordinate represents the predicted category. The elements on the diagonal represent the number of samples correctly classified, while the off-diagonal elements represent the number of samples misclassified. The 1D-FLCNN model demonstrates the highest accuracy among the models, whereas the other models show notably poorer performance in recognizing the nobody time series, as depicted in Fig. 9. Comparing the confusion matrices reveals that the 1D-FLCNN model provides the most effective recognition of bed-exit intention time series in this study.

Local features

The distribution matrix P of a randomly selected lie-down posture was performed to similarity matching experiments with feature points matrices P_i for bed-exit postures, to evaluate the accuracy of the similarity matching. The matching results are shown in Fig. 10. The x-axis represents the elements of the feature point matrix, and the y-axis represents the internal pressure values. The experimental results indicate that the
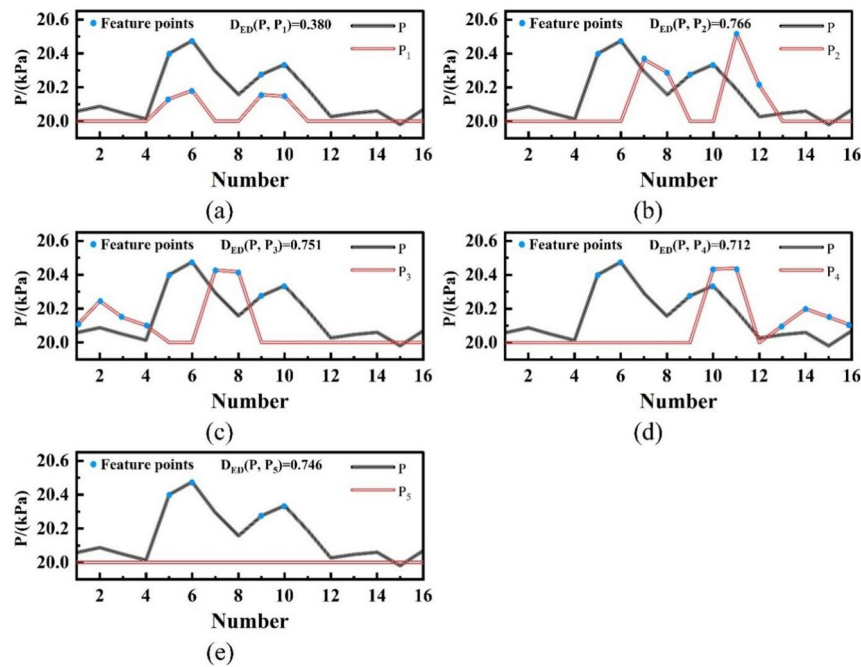
Fig. 10. The Euclidean distance of postures (**a**) Lie-down (**b**) Backpart-lifting (**c**) Right turn-back (**d**) Left turn-back (**e**) Out-of-bed.

distance $D_{ED}(P, P_1)$ between the distribution matrix P and the lie-down feature points matrix P_1 is the smallest, significantly lower than the distances to the feature points matrices for other postures, demonstrating superior matching performance.

The similarity measurement result S_m is formed into the posture sequence S_t based on their order of occurrence, as depicted in Eq. (16).

$$S_m = i = \min[D_{ED}(P, P_i)] \tag{15}$$

$$S_t = [S_1, S_2, ..., S_m] \tag{16}$$

In the detection of bed-exit state, six distinct posture sequences are defined as follows: $S_1 = [1, 2]$, $S_2 = [1, 2, 3]$, $S_3 = [1, 2, 4]$, $S_4 = [1, 2, 3, 5]$, $S_5 = [1, 2, 4, 5]$, $S_6 = [1, 5]$. In these sequences, 1 denotes lie-down, 2 represents backpart-lifting, 3 signifies right turn-back, 4 indicates left turn-back, and 5 corresponds to out-of-bed. Specifically, the S_1 posture sequence represents a general bed-exit intention. The S_2 and S_3 posture sequences convey a strong bed-exit intention. The S_4 and S_5 posture sequences indicate that the user has already left the bed. Lastly, the S_6 posture sequence suggests that a fall event has occurred.

The method based on internal pressure feature points pattern matching enables fast real-time posture recognition in a dynamic environment, catering to the demands of rapid response for real-time applications. Since it matches the local features of the internal pressure distribution of the array air springs, it can effectively avoid environmental disturbances and compensate for the shortcomings of the global feature recognition method.

Verification experiment

In this paper, the proposed method uses a combination of global and local features of the air spring internal pressure. To verify the effectiveness and anti-interference ability of this method, the ten experimenters were recruited to conduct relevant experiments. The primary goal was to verify the accuracy of identifying bed-exit intention using the methods of local feature, global feature, and a combination of local and global feature in different special environments, respectively. In the experimental environment, normal conditions refer to the participant lying in the center of the bed without any external disturbances. The special positions refer to edge positions assumed by the participants during the experiment, deviating from the normal process. Special environments simulate real-life scenarios, including irregular movements in bed and disturbances caused by objects on the bed. Each environment was tested 100 times, totaling 400 experiments. The accuracy rates of the three methods for detecting bed-exit intention were statistically analyzed, with the results presented in Table 4.

The experimental results for specific positions demonstrated that the accuracy of bed-exit intention identification using the local feature method was 83%. Meanwhile, the combined local and global feature method was 95%, indicating that this method effectively addresses the problem of failure to recognize in specific positions. The local features method is significantly influenced by body position but minimally affected by the environment.

Experimental factors	Local feature	Global feature	Local and Global feature
Normal conditions	94.00%	98.00%	96.00%
Special body positions	83.00%	97.00%	95.00%
Special environments	93.00%	86.00%	92.00%
Special environments and body positions	81.00%	87.00%	91.00%
All environments	87.75%	92.00%	93.50%

Table 4.. Verification experiment of bed-exit intention.

Ref	Recognize status /positions	Accuracy	Algorithm	Type of sensors
[12]	5	96.8%	Nonlinear support vector machine (NSVM)	Pressure sensor
[13]	4	89.0%	Histogram of oriented gradient (HOG) + Principal component analysis (PCA)	Thermopile array sensors
[16]	4	89.0%	Multilayer perceptron machine learning	Pressure sensor
[17]	3	95.0%	Yolov4-tiny	Monocular camera
[19]	3	99.2%	LSTM	Monocular camera
[21]	3	98.0%	SVM	Vibration sensors
[26]	7	93.5%	Threshold-based algorithms (TBA)	Pressure sensor
[28]	3	97.8%	Neural network (NN) + Bayesian network	Pressure and IMU sensors
[29]	5	95.0%	Madgwick algorithm + Finite-state machine (FSM)	Wearable sensors
Ours	4	93.5%	1D-FLCNN + Feature point matching	Air pressure sensors

Table 5. Comparison with other research methods.

In contrast, the experimental results obtained in specific environments indicated an accuracy of 86% in identifying the bed-exit intention using the global feature method. Additionally, the combined local and global feature method achieved an accuracy of 92%, effectively alleviating the issue of recognition errors in specific environments. The global features method is more susceptible to interference from the environment while experiencing less interference from body position.

From the above experimental results, the method combination of global features and local features can effectively avoid the influence of location and environment, address the limitations of single-feature recognition, and enhance the recognition of bed-exit intention with an accuracy of 93.5%.

Discussion

This paper innovatively proposes a bed-exit intention recognition method based on an array air spring mattress. For the field of bed-exit intention recognition, the comparison between the proposed research method and other research methods is shown in Table 5. Current approaches in bed-exit intent recognition primarily involve flexible sensors, wearable sensors, and machine vision. This paper proposes a bed-exit intention recognition method based on an array air spring mattress. Current approaches in bed-exit intent recognition primarily involve flexible sensors, wearable sensors, and machine vision. Compared to other systems, the method proposed in this paper exhibits significant advantages in multiple aspects. It completes the gap in the field of bed-exit intention recognition in air-spring rehabilitation aids and provides valuable insights for its development. Technologically, the proposed method integrates convolutional neural networks and feature point matching techniques. It can not only capture the global features of pressure distribution on the air spring mattress but also detect local features, realizing comprehensive recognition of bed-exit intention postures and states. It improves the anti-interference capability and effectively avoids the problem of non-recognition due to body position and external environment. In terms of cost, the production and deployment of air spring mattresses are relatively

lower compared to traditional flexible pressure sensor[12,16]methods. This is due to the simplified manufacturing process of the air spring mattress, low material cost, low maintenance and use cost, durability, and no frequent maintenance calibration. Our method does not require patients to wear any devices or additional sensors, significantly improving patient comfort. Traditional wearable sensors[20,29]may affect sleep quality and comfort. Additionally, the contactless recognition of bed-exit intentions using the air spring mattress avoids the use of cameras and other devices that could raise privacy concerns. Compared to machine vision[14,17–19] methods, this approach mitigates potential privacy issues, making it more suitable for environments with high privacy requirements.

Nevertheless, challenges such as interpreting internal pressure changes and managing device complexity remain for our method. Future research will further explore the influence of environmental factors on internal pressure changes, optimize the design of arrayed air spring mattresses and sensor layouts, and simplify the devices to enhance usability.

Conclusion
This paper explores a method for recognizing bed-exit intention based on internal pressures features of the array air springs. The method utilizes 1D-FLCNN to identify the global features of the internal pressure and employs feature points matching technique to recognize the local features of the internal pressure distribution. The proposed 1D-FLCNN sample classification model, based on FL and 1D-CNN, effectively classifies eight different internal pressure time series. Additionally, the feature point matching method can identify five bed-exit postures according to the pressure distribution characteristics of the array air spring. This recognition method combines global features and local features to realize the comprehensive recognition of bed-exit intention. Experimental validation confirms that the proposed method greatly improves the anti-interference capability and effectively avoids the problem of non-recognition due to body position and external environment. This study improves the nursing system based on smart nursing mattresses and provides valuable insights for the development of intention recognition in air-spring rehabilitation aids.

Data availability
The data that support the findings of this study are available from the corresponding author upon reasonable request.

References
1. Beauchet, O., Matskiv, J., Rolland, Y., Schott, A. M. & Allali, G. ER2 risk levels and their association with incident falls, their recurrence and post-fall fractures in older women: Results of the EPIDOS study. *Maturitas* **178**, 107838 (2023).
2. Beauchet, O., Matskiv, J., Rolland, Y., Schott, A. M. & Allali, G. Interaction between cognitive and motor disorders for risk screening of incident falls: results of an elderly population-based observational cohort study. *Aging Clin. Exp. Res.* **35**(5), 1027–1032 (2023).
3. Alanazi, F. K., Lapkin, S., Molloy, L. & Sim, J. The impact of safety culture, quality of care, missed care and nurse staffing on patient falls: A multisource association study. *J. Clin. Nurs.* **32**(19–20), 7260–7272 (2023).
4. Yu, W. Y., Hwang, H. F. & Lin, M. R. Gender differences in personal and situational risk factors for traumatic brain injury among older adults. *J. Head Trauma Rehabil.* **37**(4), 220–229 (2022).
5. Wah, W., Berecki-Gisolf, J. & Walker-Bone, K. Epidemiology of work-related fall injuries resulting in hospitalisation: individual and work risk factors and severity. *Occup. Environ. Med.* **81**(2), 66–73 (2024).
6. Liu, C., Xu, T., Xia, W., Xu, S., Zhu, Z., Zhou, M., et al. Incidence, prevalence, and causes of spinal injuries in China, 1990–2019: Findings from the Global Burden of Disease Study 2019. Chin. Med. J. 10–1097 (2024).
7. Goddard, K. S., Hall, J. P., Greiman, L., Koon, L. M., Gray, R. C. Examining the effects of home modifications on perceptions of exertion and safety among people with mobility disabilities. Disabil. Health J. 101590 (2024).
8. Sullivan, R., Harding, K., Skinner, I. & Hemsley, B. Falls in patients with communication disability secondary to stroke. *Clin. Nurs. Res.* **32**(3), 478–489 (2023).
9. Chao, Y., Liu, T. & Shen, L. M. Method of recognizing sleep postures based on air pressure sensor and convolutional neural network: For an air spring mattress. *Eng. Appl. Artif. Intell.* **121**, 106009 (2023).
10. Li, Z., Zhou, Y. & Zhou, G. A dual fusion recognition model for sleep posture based on air mattress pressure detection. *Sci. Rep.* **14**(1), 11084 (2024).
11. Lin, C. L., Sun, Z. T. & Chen, Y. Y. Air-mattress system for ballistocardiogram-based heart rate and breathing rate estimation. *Heliyon* **9**(1), e12717 (2023).
12. Duan, B. W., Zhao, D. H., Yang, J. Y. & Wang, S. Y. A Novel Posture Recognition Based on Time Series Supervised Learning Algorithm. *Proceedings of the IEEE International Conference on Intelligence and Safety for Robotics.* **2021**, 394–398 (2021).
13. Chen, Z. J. & Wang, Y. Remote recognition of in-bed postures using a thermopile array sensor with machine learning. *IEEE Sens. J.* **21**(9), 10428–10436 (2021).
14. Ishizu, F., Tajima, T., Abe, T. Analysis and Prediction of Patient Falls from Beds Using an Infrared Depth Sensor. Sens. Mater. 35 (2023).
15. Emilsson, M., Karlsson, C. & Svensson, A. Experiences of using surveillance cameras as a monitoring solution at nursing homes: The eldercare personnel's perspectives. *BMC Health Serv Res.* **23**(1), 144 (2023).
16. Bai, D. Y., Ho, M. C., Mathunjwa, B. M. & Hsu, Y. L. Deriving multiple-layer information from a motion-sensing mattress for precision care. *Sensors* **23**(3), 1736 (2023).
17. Lin, C. J., Wei, T. S., Liu, P. T., Chen, B. H. & Shi, C. H. Bed-exit behavior recognition for real-time images within limited range. *Sensors* **22**(15), 5495 (2022).
18. Gutiérrez, J. et al. Fall Detection in Low-Illumination Environments From Far-Infrared Images Using Pose Detection and Dynamic Descriptors. *IEEE Access.* **12**, 41659–41675 (2024).
19. Inoue, M. & Taguchi, R. Bed exit action detection based on patient posture with long short-term memory. *IEEE Eng. Med. Biol. Soc.* **2020**, 4390–4393 (2020).
20. Zhang, G. Q., Li, P., Wang, X., Xia, Y. S. & Yang, J. Flexible battery-free wireless sensor array based on functional gradient-structured wood for pressure and temperature monitoring. *Adv. Funct. Mater.* **33**(2), 2208900 (2023).

21. Valero, M., Clemente, J., Li, F. Y. & Song, W. Z. Health and sleep nursing assistant for real-time, contactless, and non-invasive monitoring. *Pervasive Mob. Comput.* **75**, 101422 (2021).
22. Guo, T. et al. Dual-view spectral and global spatial feature fusion network for hyperspectral image classification. *IEEE Trans. Geosci. Remote Sensing* **61**, 5512913 (2023).
23. Yan, L. Y., Shi, Y., Wei, M. H. & Wu, Y. L. Multi-feature fusing local directional ternary pattern for facial expressions signal recognition based on video communication system. *Alex. Eng. J.* **63**, 307–320 (2022).
24. Zhang, Y. et al. A flexible turning and sensing system for pressure ulcers prevention. *Electronics* **10**(23), 2971 (2021).
25. Scalise, C. et al. Hospital restraints: safe or dangerous? A case of hospital death due to asphyxia from the use of mechanical restraints. *Int. J. Environ. Res. Public Health* **19**(14), 8432 (2022).
26. Ruiz, J. F. B. et al. Bedtime monitoring for fall detection and prevention in older adults. *Int. J. Environ. Res. Public Health* **19**(12), 7139 (2022).
27. Lin, W. Y., Chen, C. H. & Lee, M. Y. Design and implementation of a wearable accelerometer-based motion/tilt sensing internet of things module and its application to bed fall prevention. *Biosensors-Basel* **11**(11), 428 (2021).
28. Viriyavit, W. & Sornlertlamvanich, V. Bed position classification by a neural network and bayesian network using noninvasive sensors for fall prevention. *J. Sens.* **2020**, 5689860 (2020).
29. Lin, H. C., Chen, M. J., Lee, C. H., Kung, L. C. & Huang, J. T. Fall recognition based on an IMU wearable device and fall verification through a smart speaker and the IoT. *Sensors* **23**(12), 5472 (2023).
30. Woltsche, R., Mullan, L., Wynter, K. & Rasmussen, B. Preventing patient falls overnight using video monitoring: a clinical evaluation. *Int. J. Environ. Res. Public Health* **19**(21), 13735 (2022).
31. Ige, A. O. & Noor, M. H. M. A deep local-temporal architecture with attention for lightweight human activity recognition. *Appl. Soft. Comput.* **149**, 110954 (2023).
32. Seow, J. P., Chua, T. L., Aloweni, F., Lim, S. H. & Ang, S. Y. Effectiveness of an integrated three-mode bed exit alarm system in reducing inpatient falls within an acute care setting. *Jpn. J. Nurs. Sci.* **19**(1), e12446 (2022).
33. Miyake, N., Shibukawa, S., Masaki, H. & Otake-Matsuura, M. User-oriented design of active monitoring bedside agent for older adults to prevent falls. *J. Intell. Robot. Syst.* **98**(1), 71–84 (2020).
34. Xu, H., Tian, Y., Ren, H. & Liu, X. A Lightweight Channel and Time Attention Enhanced 1D CNN Model for Environmental Sound Classification. *Expert Syst. Appl.* **249**, 123768 (2024).
35. Choi, J. G., Kim, D. C., Chung, M., Lim, S. & Park, H. W. Multimodal 1D CNN for delamination prediction in CFRP drilling process with industrial robots. *Comput. Ind. Eng.* **190**, 110074 (2024).
36. Flower, T. M. L. & Jaya, T. A novel concatenated 1D-CNN model for speech emotion recognition. *Biomed. Signal Process. Control.* **93**, 106201 (2024).
37. Lin, T. Y., Goyal, P., Girshick, R., He, K. & Dollar, P. Focal loss for dense object detection. *IEEE Trans. Pattern Anal. Mach. Intell.* **42**(2), 18–327 (2020).
38. Thuy, H. T. T., Anh, D. T. & Chau, V. T. N. Efficient segmentation-based methods for anomaly detection in static and streaming time series under dynamic time warping. *J. Intell. Inf. Syst.* **56**(1), 121–146 (2021).
39. Guigou, F., Collet, P. & Parrend, P. SCHEDA: Lightweight euclidean-like heuristics for anomaly detection in periodic time series. *Appl. Soft. Comput.* **82**(3), 1432–1443 (2019).
40. Montagnon, C. F. Forecasting by splitting a time series using Singular Value Decomposition then using both ARMA and a Fokker Planck equation. *Physica A* **567**(3), 536–545 (2021).

Author contributions

F. M.: Conceptualization, Methodology, Software, Data curation, Writing—original draft, Experimental platform construction. T. L.: Conceptualization, Methodology, Formal analysis, Writing review & editing. C. M.: Investigation, Methodology. J. Z.: Methodology, Supervision. Y. Z.: Methodology, Software. S. G.: Conceptualization, Formal analysis. All authors approved the final manuscript and were accountable for the study, ensuring that data generated or analyzed in this study are available.

Funding

Declaration

Competing interests

The authors declare that they have no known competing financial interests or personal relationships that could have appeared to influence the work reported in this paper.

Ethics approval and consent to participate

All methods were performed in accordance with the Declaration of Helsinki. This study was approved by the Ethics Committee of Hebei University of Technology Approval (Approval No. HEBUThMEC2023019). Informed consent has been obtained from all subjects and/or their legal guardians.

Additional information

Correspondence and requests for materials should be addressed to T.L.

Reprints and permissions information is available at www.nature.com/reprints.

Publisher's note Springer Nature remains neutral with regard to jurisdictional claims in published maps and institutional affiliations.